Information Patterns and Hedging Brockett's Theorem in Controlling Vehicle Formations

J. Baillieul* A. Suri*

February, 2003

Abstract

Efforts to apply computer vision and various optical and acoustic proximity sensors for distributed/ coordinated motion control of a small group of autonomous vehicles has led us to consider a number natural feedback control laws which utilize realtime measurements of relative distances between the vehicles. Unfortunately, none of the feedback laws satisfies Brockett's necessary conditions for asymptotic stabilization. They *do* appear to provide a basis for practical solutions to a number of interesting vehicle control problems, however. Part of the rationale for proposing feedback laws which are not asymptotically stabilizing is that in a number of cases of practical interest, one may show that the set of initial conditions which are not driven to the prescribed rest point is either small (in some sense) or uninteresting (in the problem context) or both. In some cases, one can also show that by choosing feedback gains in terms of the problem's initial conditions—using say a table look-up—it is possible to steer from any given initial state into an arbitrarily small neighborhood of the desired goal state. The aim of the research here is to develop a large catalogue of simple controlled motions which in appropriate sequential combinations permit autonomous nonholonomic vehicles to assemble themselves and execute coordinated motions in highly structured formations.

Keywords: formation framework, rigid formation, leader first-follower pair, constructive rigidity

1 Introduction

This paper is concerned with the interplay between nonlinear control designs and the problem of coordinated motion control of groups of robot vehicles. The discussion is largely guided by recent experiments with a group of laboratory robots, where the information needed in real-time for motion control is gained from a variety of sensors including sonar, active vision, laser range finders, GPS, and so forth. An important open problem in controlling group motions of highly instrumented robots is that of registering and reconciling real-time sensor data. The central problem we treat here, however, concerns the use of available data from sensors to control nonholonomically constrained motions of (possibly large) groups of vehicles. The paper consists of two interrelated parts: the first dealing with basic concepts of the stability of formations and the second treating methods of achieving stable formations by groups of vehicles whose motions are subject to nonholonomic constraints.

*Dept. of Aerospace and Mechanical Engineering, Boston University, Boston, MA 02215. E-mail: johnb@bu.edu Both authors gratefully acknowledge support from the Army Research Office under the ODDR&E MURI97 Program Grant No. DAAG55-97-1-0114 to the Center for Dynamics and Control of Smart Structures (through Harvard University) and from ODDR&E MURI01 Program Grant Number DAAD19-01-1-0465 to Boston University and the Center for Networked Communicating Control Systems.

The stability analysis of motions of vehicle formations has followed several distinct paths in the recent literature. A number of researchers have worked to extend classical robot navigation methods based on the use of synthetic potentials and motions based on gradient descent. (See, for instance, [13] and [12].) Lian and Murray have discussed the use of a Nonlinear Trajectory Generation (NTG) algorithm tailored to the special needs of multivehicle formation motions, [15]. The recent work of Tanner, Pappas, and Kumar ([18]) considers the problem of *input-to-state* stability for interconnected systems, and discusses ways in which the stability of a formation may be assessed in terms of knowledge of primitive component graphs. The work of Eren, Belhumeur, and Morse ([6]) shows how tightly structured formation control may be discussed in terms of the theory of graph rigidity (See [7] and [8] for the basics of this theory.). In the work described below, we make contact with both these approaches. We consider formation motions of two classes of mobile robot vehicle models. Both are idealizations of the real world, but they both provide models which can be analyzed and which provide guiding principles for actual implementations of distributed control laws. The simplest models involve what we shall call *holonomic point vehicles*—or *point vehicles* for short. Each vehicle is modeled as a point which undergoes *holonomic* motion (in the plane or in space). Using localized relative distance control, it is shown how stable motions of individual vehicles may be used together with selected patterns of local feedback to produce stable formations. Making contact with the classical theorem of Henneberg, we show that essentially the only stable formation graphs are those which are constructible by a sequence of rigid vertex extensions. The result is of particular interest because it defines the class of possible formations which are stable under local relative position feedback, and it points immediately to a control strategy for having autonomous robot vehicles assemble themselves into any of these formations.

In the other class of models treated below, all vehicles are modeled as *nonholonomic skates*. These are also idealizations of the physical world, but they allow us to examine how the essential features of graph-based theories of formation motions must be adapted to account for nonholonomic constraints on the motions of component vehicles.

The paper is organized as follows. In Section 2, we introduce terminology needed to discuss formation graphs. Section 3 presents basic results on the theory of rigid formation stability for the case of point vehicles. The main idea is that certain patterns of relative proximity information are required to ensure stable formations. It is shown that essentially the only stable rigid formations are obtained through a constructive procedure starting with a *leader-first-follower* pair. All the results of Section 3 are established for the case of point vehicles, but they serve to motivate the class of nonholonomic vehicle control laws discussed in Section 4. All the control laws use simple relative proximity feedback in different ways. Because they generally fail to satisfy Brockett's necessary conditions, asymptotic stability results are not possible. It is shown, however, that by carefully tuning the feedback laws to the measured operating conditions, stable performance can be guaranteed which meets the design objectives on very thin and easily specified sets. In Section 5, we present our conclusions, emphasizing that the set of control laws described in Section 4 must be further enlarged to provide an adequately rich set of motion options to create the stable formation patterns described in Section 3.

2 Formation graphs

It is useful to discuss the controlled motions of multiple robots in terms of the level of coordination involved. The following terminology will help organize this discussion.

Definition 1 A *squadron configuration* is an element $(q_1, \ldots, q_n)$ in a finite product $\mathrm{SE}(m, \mathbb{R}) \times \cdots \times \mathrm{SE}(m, \mathbb{R})$ of copies of the Euclidean group where $m = 2$ or 3. □

Definition 2 A *formation graph* $\mathcal{G}$ is a pair $\mathcal{G} = (\mathcal{S}, E)$ where $\mathcal{S}$ is a finite vertex set, $\{s_1, s_2, \ldots, s_n\}$, in one-to-one correspondence with n elements (configurations) $q_j \in \mathrm{SE}(m, \mathbb{R})$, and where $E \subseteq \mathcal{S} \times \mathcal{S}$ is a set of

directed edges $\varepsilon_{ij} = \varepsilon(q_i, q_j)$ specifying associations among pairs of vertices and the configurations to which they correspond. □

Given a formation graph $(\mathcal{S}, E)$, let e be the cardinality of the edge set E. Admitting the possibility that E is the empty set, it is obvious that $0 \leq e \leq \binom{n}{2}$.

Definition 3 A *formation framework* $(\mathcal{S}, E, \mathbf{q})$ consists of a formation graph $(\mathcal{S}, E)$ and a function $\mathbf{q}$ from the vertex set $\mathcal{S}$ into the squadron configuration space $\mathrm{SE}(m, \mathbb{R}) \times \cdots \times \mathrm{SE}(m, \mathbb{R})$. □

It will frequently be convenient to blur the distinction between $\mathcal{S}$ and the set of configurations $\{q_1, \ldots, q_n\}$ to which it corresponds under the mapping $\mathbf{q}$.

Definition 4 A *formation specification* is a labeling of the edges $\varepsilon_{ij} \in E$ of the formation graph by elements in appropriate subgroups $H_{ij} \subset \mathrm{SE}(m, \mathbb{R})$ such that for each $\varepsilon_{ij} \in E$, H_{ij} is a fixed subgroup of one of the ten known types of Lie subgroups of $\mathrm{SE}(3, \mathbb{R})$. (See [16] for details on the lattice of Lie subgroup types.) For each squadron configuration, a formation specification assigns values $F_{ij} = F_{ij}(q_i, q_j) \in H_{ij}$. □

We think of each entry q_j in a squadron configuration $(q_1, \ldots, q_n)$ as a pair R_j, r_j where R_j is an element of the rotation group $\mathrm{SO}(m)$ and $r_j \in \mathbb{R}^m$, for $m = 2$ or 3. Formation specification functions take values in subgroups $H_{ij} \subset \mathrm{SE}(m, \mathbb{R})$ which may naturally be thought of as specifying relative position information regarding the $i-$th and $j-$th nodes. We emphasize the important special case in which $H_{ij} = \mathbb{R}$, however, in which real number data of any kind can be used to label a formation graph.

The special case of *point vehicles***.** A complete theory of motions of groups of vehicles in either the plane or in space must capture the details of interrelationships between configurations in $\mathrm{SE}(m, \mathbb{R})$, for $m = 2$ or 3 respectively. This will be especially important in describing group motions of vehicles subject to nonholonomic constraints. Nevertheless, there is an interesting part of the theory in which the configuration space of each vehicle may be taken to be simply $\mathbb{R}^2$ or $\mathbb{R}^3$. We use parallel terminology as needed: A *point vehicle squadron configuration* is an element $(q_1, \ldots, q_n) \in \mathbb{R}^m \times \ldots \times \mathbb{R}^m$, where $m = 2$ or 3, with corresponding definitions of *point vehicle formation graph*, *point vehicle formation framework*, and *point vehicle formation specification* involving the appropriate parallel modifications.

Examples (i) A useful formation specification is given by associating to each $\varepsilon_{ij} \in E$ the Euclidean distance $d_{ij} = \|r_i - r_j\|$ between corresponding configurations. In the case of sensor-labeled graphs, we have $d_{ij} = \|r_i - r_j\| + n_{ij}$, where n_{ij} is a variable sensor noise, sensor bias, etc. Since sensing is being done in a distributed fashion, with each sensor subject to noise and bias, we do not assume that $d_{ij} = d_{ji}$.

(ii) For formations of vehicles modeled as having positive spatial extent, an interesting formation specification is given by associating to each $\varepsilon_{ij} \in E$ the corresponding relative orientation $R_i R_j^{-1}$. Such specifications are of interest in describing group motions of flocks of birds and schools of fish. (See e.g. [3], [10], and [11].)

The idea of a formation graph is closely related to the idea of a Euclidean graph proposed earlier by Brockett ([2]), but in our formulation, we do not impose the consistency conditions of Brockett. Similar ideas have also appeared recently in several places in the rapidly growing body of research on motions of groups of robots. See Das *et al.* [5] for ideas bearing the greatest similarity.

Given a formation specification $F = \{F_{ij}\}$ where $F_{ij} = F_{ij}(q_i, q_j) \in H_{ij}$, a *formation motion* is defined to be a curve $q(t) = \big(q_1(t), \ldots, q_n(t)\big)$, $0 \leq t \leq t_f$ in $\mathrm{SE}(m, \mathbb{R})^n$ along which F is constant. We are interested in the real-time information processing that must be carried out in order to maintain a given formation. An interesting special class of formation motions is associated with the relative distance constraint function $F_{ij}(q_1, \ldots, q_n) = \|r_i - r_j\|$. For this class of formation specifications, the case in which *all* $\binom{n}{2}$ relative distances $\|r_i - r_j\|$ remain constant is of special interest.

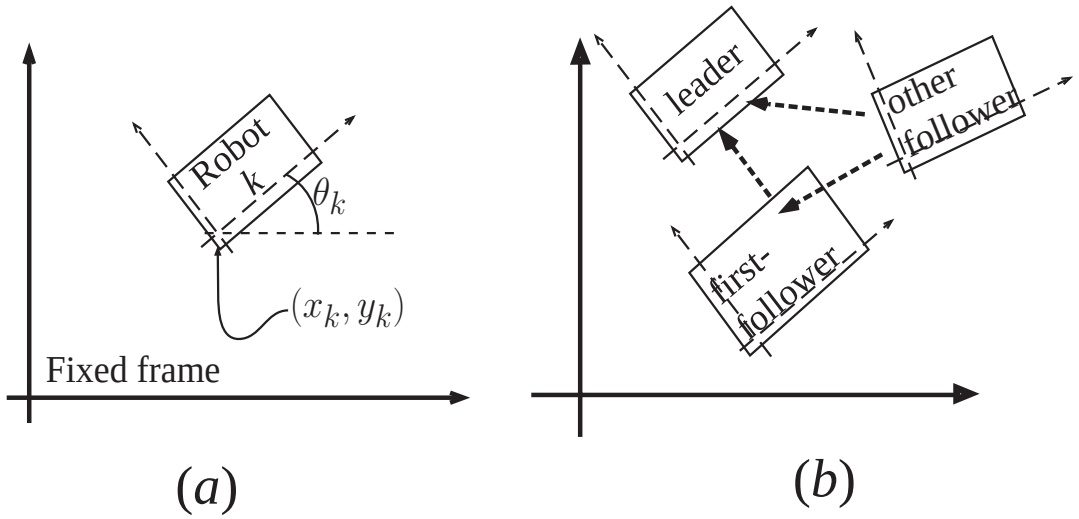

Figure 1: (a) A planar mobile robot's configuration is prescribed by body coordinates (x_k, y_k, θ_k). (b) In formations involving multiple robots, follower robots determine their positions with respect to a "leader" or "leader-follower" pair.

Definition 5 Motions which preserve all pairs of relative distances $\|r_i - r_j\|$ are called *rigid motions* of the framework. □

In the next section, we shall describe conditions under which distributed control can be applied to keep rigid formations (statically) stable.

3 Stably rigid formations of point vehicles

The idea of rigidly maintaining pairwise constant distances between members of a formation has been extensively explored in the case robot vehicles are idealized to be points in Eren, Belhumeur, and Morse [6]. The analysis relies heavily on ideas from classical Euclidean geometry, as well as current results from contemporary rigidity theory and structural topology. (See, for instance, [7].) In our development, we shall be principally concerned with the case in which the robot vehicles move subject to nonholonomic constraints. We begin, however, by studying the simpler case of rigid formations of point vehicles. This setting illuminates important details of the consequences of the intervehicle distances being measured in a distributed fashion by sensors which are subject to noise. Our aim is to develop formation specifications which imply rigidity and which are in some sense minimal.

Vehicle formations based on distributed sensing. Consider, for instance, the problem of rigidly maintaining a triangular formation of three robot vehicles. Suppose each of three robots A, B, and C has the capability of sensing distance and line-of-sight direction to neighboring robots using sensors which may include sonar, active IR, laser range finders, or stereo vision. As depicted in Figure 2, we draw arrows

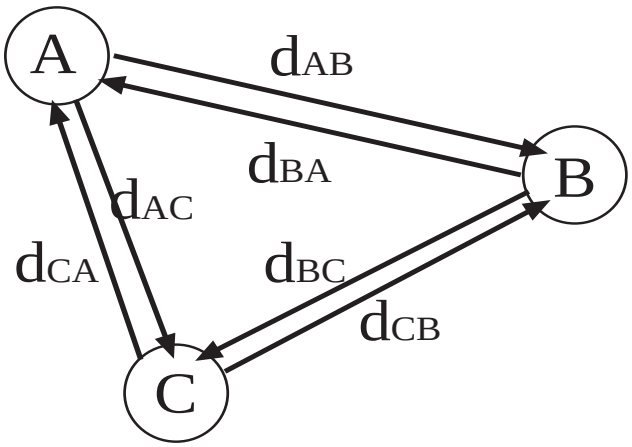

Figure 2: A triangular formation determined by sensor measurements. Each of three mobile robots can sense the distance to its two neighbors, and also the angles between the line-of-sight vectors to the neighbors. The labels on the arrows - e.g. d_{AB} - denote the distance from A to B as measured by an active sensor (e.g. sonar) on the robot at the base of the arrow.

between pairs of robots in the formation and label each arrow with the distance measured from the robot at the base of the arrow. The measurements needed to determine whether the robots are in the prescribed formation are thus made in a distributed fashion. It is clearly not necessary for every robot to know all the dimensions of the triangle being formed, but each robot needs to be able to verify and communicate that it is at the prescribed distance from its neighbors. Because each distance measurement can be made by more than one robot, triangular formations can be robustly maintained in the face of sensor failures. If the robots are able to communicate, then in the worst case of sensor failure, a single robot with working sensors can guide the other two to their required positions in the triangle.

There is a problem with trying to integrate such redundant sensor data, however. In the ideal case of perfect measurements, we would have $d_{AB} = d_{BA}$ (refer to Figure 2), but in the real world of noisy sensors and otherwise faulty measurements, we cannot assume this. An interesting consequence of the measured distance d_{AB} being unequal to the measured distance d_{BA} is that decentralized, non-communicating position control is inherently unstable. Assume (without loss of generality) that the measured distance $d_{AB} > d_{BA}$. If the two robots A and B are programmed to move to have a specified separation, A will try to move closer to B, while B will try to move away from A (because of the difference in the measured values of the distance). Without additional compensating control, the two robots will thus push and pull each other out from any preassigned neighborhood in their shared workspace. We shall refer to this type of instability which is due to unreconciled differences in real-time data from distributed sensors as an *information-based instability.*

Two simple approaches to controlling this instability are

1. Have only one of the two robots actively control the separation distance while the other remains passive, and

2. Have the robots communicate to each other their respective distance measurements and appropriately compensate for the sensor misregistration.

Of these solutions, the first is considerably simpler because it does not require real-time communication of sensor data over a noisy and possibly congested communications channel. Nevertheless, both approaches will be of interest, and we find it useful to distinguish two formation control strategies accordingly.

Terminology: (i) We shall use the term *sensor-mediated* formation control to refer to the class of distributed feedback control laws in which each robot controls its own position based only on data available from its own on-board sensors. (ii) The term *communications-mediated* formation control refers to the class of distributed feedback laws in which some of the robots in the formation control their positions using data which is acquired from sensors on other robots in the formation and transmitted over a communications link. □

Consider the problem of configuring three robots into a prescribed triangular shape based on sensor-measured relative distances. Two possible distance sensing strategies are depicted in Figure 3. In Figure 3(a), each robot senses its distance to a neighbor in the cyclic pattern depicted. If the robots are able to communicate with each other, the distance measurements can be shared to determine whether they are in the prescribed formation. Without communication among the vehicles, stable motions to bring about the desired formation cannot be achieved using this pattern of sensor feedback, however. This may be seen in terms of a simple model of controlled formation motions in which the robot coordinates are idealized to be points —with planar coordinates $(x_1, y_1), (x_2, y_2)$, and (x_3, y_3). The general form of a first-order (kinematic) model based on relative distance measurements associated with the sensor pattern depicted in Figure 3(a) is

$$\begin{pmatrix} \dot{x}_1 \\ \dot{y}_1 \\ \dot{x}_2 \\ \dot{y}_2 \\ \dot{x}_3 \\ \dot{y}_3 \end{pmatrix} = \begin{pmatrix} f_1(x_1 - x_3, y_1 - y_3) \\ g_1(x_1 - x_3, y_1 - y_3) \\ f_2(x_2 - x_1, y_2 - y_1) \\ g_2(x_2 - x_1, y_2 - y_1) \\ f_3(x_3 - x_2, y_3 - y_2) \\ g_3(x_3 - x_2, y_3 - y_2) \end{pmatrix}. \tag{1}$$

The linearization of this vector-field about any point involves a matrix of partial derivatives which can easily be shown to have two zero eigenvalues, eliminating the possibility of asymptotically stable motions. □

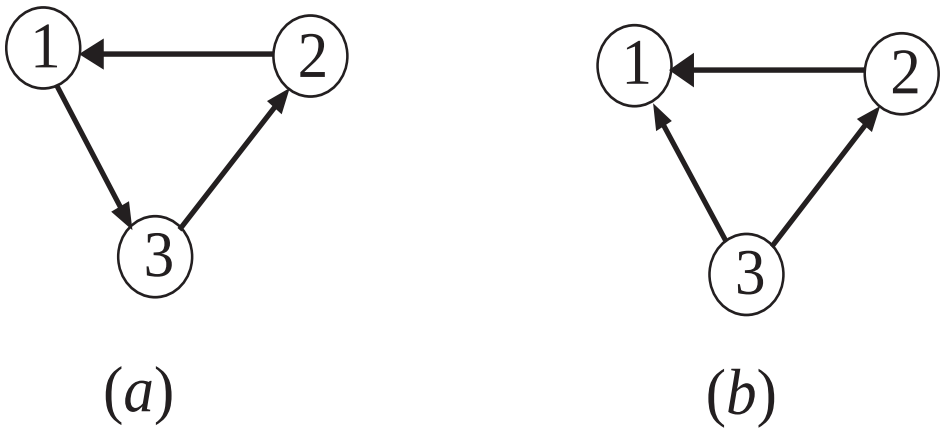

Figure 3: There is enough combined sensor information to determine whether the three robots are in a prescribed triangular configuration in either case. In case (a), there is no way for the robots to configure themselves in the prescribed configuration without communication. In case (b), however, robot 2 can use only it's local sensor data to position itself the prescribed distance from robot 1, and then robot 3 can use only its own sensor information to position itself the prescribed distances from both 1 and 2.

Remark 1 *On the unstable motions associated with cyclic sensing of relative positions.* The instabilities that result from such cyclic sensing patterns are similar to—but richer than—the previously described

information-based instabilities. The motions of (1) will typically have asymptotic limiting behaviors whose gross qualitative features depend strongly on the initial configurations of the formation and for which there is a limiting steady state motion/configuration which can only be determined by integrating the differential equation. A special case which illustrates the possibilities is the first-order relative distance control law defined by

$$\begin{pmatrix} \dot{x}_i \\ \dot{y}_i \end{pmatrix} = \left[d_i - \sqrt{(x_i - x_j)^2 + y_i - y_j)^2} \right] \begin{pmatrix} x_i - x_j \\ y_i - y_j \end{pmatrix} \tag{2}$$

for $(i, j) = (1, 3), (2, 1)$, and $(3, 2)$. This is an easily implementable kinematic control law using relative distance measurements between the i-th and j-th robot vehicles. There are two easily identifiable asymptotic limiting behaviors. In one typical behavior, (corresponding to an open set of initial conditions), the three points $(x_i(t), y_i(t))$ approach a stationary triangular configuration with coordinate values satisfying

$$d_i - \sqrt{(x_i - x_j)^2 + y_i - y_j)^2} = 0, \quad \text{for } (i, j) = (1, 3), (2, 1), (3, 2).$$

The solution set of this system of equations is a subvariety of $\mathbb{R}^6$ having dimension 3, reflecting the fact that these equations do not determine either the position or orientation of the triangle whose shape they characterize. This indeterminacy is the essential feature of one form of instability associated with a cyclic pattern of distributed relative distance sensing.

Another limiting behavior observed for the motions of (2) is one in which all points move at the same (non-zero) velocity and are aligned one behind the other. In this case, $\dot{x}_1 = \dot{x}_2 = \dot{x}_3 \neq 0$, and $\dot{y}_1 = \dot{y}_2 = \dot{y}_3 \neq 0$. This manifestation of instability is similar to the information-based instability discussed above. Again, there is an open set of initial conditions which lead to this motion in the limit.

Stable formation motions using acyclic relative position sensing. For the problem of relative position sensing depicted in Figure 3(b), there is an obvious leader-follower hierarchy which is missing in the case of cyclic sensing. In this case, and in what follows, we resolve any indeterminacy by assuming the leader and first-follower (vehicles 1 and 2 respectively) have global position information which allows them to navigate to a prescribed configuration with respect to a fixed (world) coordinate system. Once this is done, vehicle 3 will control its position using only feedback measurements of relative proximity to vehicles 1 and 2. No similar hierarchical position control strategy will work for the case of cyclic proximity sensing. Denote the distance between vehicles 1 and 2 by d_{12}. We can place vehicle 3 at distances d_1 and d_2 respectively from vehicles 1 and 2 provided $d_1 + d_2 \geq d_{12}$. To avoid a degeneracy in which the three vehicles lie on a line, it is useful to assume that three "triangle" inequalities are satisfied:

$$d_1 + d_2 > d_{12}, \quad d_1 + d_{12} > d_2 \quad d_{12} + d_2 > d_1.$$

Under this assumption the two equations

$$\begin{aligned} &d_1 - \sqrt{(x - x_1)^2 + (y - y_1)^2} = 0 \text{ and} \\ &d_2 - \sqrt{(x - x_2)^2 + (y - y_2)^2} = 0 \end{aligned} \tag{3}$$

determine two distince possible locations of robot vehicle 3 which are each a distance d_1 and d_2 respectively from vehicles 1 and 2. We propose the following kinematic control law to move vehicle three toward one of these locations:

$$\begin{pmatrix} \dot{x} \\ \dot{y} \end{pmatrix} = \left[d_1 - \sqrt{(x - x_1)^2 + y - y_1)^2} \right] \begin{pmatrix} x - x_1 \\ y - y_1 \end{pmatrix} + \left[d_2 - \sqrt{(x - x_2)^2 + y - y_2)^2} \right] \begin{pmatrix} x - x_2 \\ y - y_2 \end{pmatrix}. \tag{4}$$

Let (x_e, y_e) be one of the two solutions to (3). This is clearly a rest point for the system (4). The linearized motion about this rest point is given by

$$\begin{pmatrix} \dot{\delta x} \\ \dot{\delta y} \end{pmatrix} = -A(x_e, y_e) \begin{pmatrix} \delta x \\ \delta y \end{pmatrix},$$

where

$$A(x_e, y_e) = \begin{pmatrix} \frac{(x_e-x_1)^2}{d_1} + \frac{(x_e-x_2)^2}{d_2} & \frac{(x_e-x_1)(y_e-y_1)}{d_1} + \frac{(x_e-x_2)(y_e-y_2}{d_2} \\ \frac{(x_e-x_1)(y_e-y_1)}{d_1} + \frac{(x_e-x_2)(y_e-y_2}{d_2} & \frac{(y_e-y_1)^2}{d_1} + \frac{(y_e-y_2)^2}{d_2} \end{pmatrix}.$$

It is straightforward to show that the matrix $A(x_e, y_e)$ has two positive eigenvalues unless the quantity $(x_e - x_1)(y_e - y_2) - (x_e - x_2)(y_e - y_1)$ vanishes. This cannot happen unless the three points (x_e, y_e), (x_1, y_1), and (x_2, y_2) are collinear, which our triangle inequality assumption has ruled out.

We have in fact shown that triangular configurations are stable under the acyclic pattern of relative position sensing depicted in Figure 3 precisely when the triangle is rigid (the case in which the three triangle inequalities are satisfied). Stable rigid formation motions thus require that we enforce the assumption that there are *no cycles* in the formation graph. Das *et al.* have previously mentioned this assumption ([5]), and it will be shown below that it is necessary, but not sufficient, to characterize stably rigid point vehicle formations.

Stable rigid vehicle formations. Consider an n-vehicle squadron in which vehicle 1 is designated to be "leader," and vehicle 2 is "first-follower" as in Figure 3. We are interested in relative motions of vehicles other than these two which result in stably rigid formations. Suppose a formation specification is given by labeling each edge $\varepsilon_{ij} \in E$ of the formation graph with a prescribed distance d_{ij} between the vehicle positions r_i and r_j. Each such edge label will have an associated direction indicating whether the distance is measured by the i-th vehicle looking at the j-th vehicle or vice-versa. To implement distributed relative distance based formation control, each vehicle in the formation will move in order to control its relative distance to all other vehicles to which there corresponds a directed edge in E. To the i-th vehicle in the formation, with associated vertex $s_i \in \mathcal{S}$, there is a corresponding set of vertices

$$J_i = \{s \in \mathcal{S} : \text{ there is a directed edge } \varepsilon \in \text{E from} s_i \text{to } s\}.$$

We shall blur the distinction between vertices in $s_i \in \mathcal{S}$ and the indices i labeling the formation vehicles to which they correspond. Using this notation, and motivated by the examples above, we introduce a general model for *distributed relative distance control* of a point vehicle formation:

$$\begin{pmatrix} \dot{x}_i \\ \dot{y}_i \end{pmatrix} = \sum_{j \in J_i} u_{ij}(d_{ij}, \sqrt{(x_i - x_j)^2 + y_i - y_j)^2}) \begin{pmatrix} x_i - x_j \\ y_i - y_j \end{pmatrix}, \quad i \neq 1, 2, \tag{5}$$

where d_{ij} is the set-point distance between vehicles i and j, and u_{ij} is thus a function of both the set-point and the measured distance. The leader ($i = 1$) and first-follower ($i = 2$) are assumed to be staionary in this analysis.

Definition 6 A formation will be said to be *stably rigid* under a control law of the form (5) if for any sufficiently small perturbation in the relative positions of the vehicles, the control law steers them asymptotically back into the prescribed formation (in which the relative distance constraints are satisfied).

In general, we would like to characterize larger stably rigid configurations (4 or more graph nodes) in which all vehicles are at prescribed positions relative to a "leader" (node 1 in Figure 3(b)) and a "first

follower" (node 2 in Figure 3(b)). With the aim of stating sufficient conditions for stable formations, we introduce a term from the classical theory of graph rigidity. We say that a formation framework $(\mathcal{S}, E, \mathbf{q})$ is *isostatic* if the removal of any edge $e \in E$ results in a framework which is not rigid. Isostatic frameworks thus have no redundant edges. They are clearly of interest because any sensor-mediated formation control which does not require sensor registration will clearly produce an isostatic formation framework. Having an isostatic formation framework is by itself not sufficient to guarantee stable formation motions, as has been seen and is illustrated by Figure 3(a) (which is isostatic but not stably rigid). Even under the dual hypothesis that a formation framework is both isostatic and acyclic, we cannot conclude that stably rigid formation motions are possible. This is easily seen by looking at the formation depicted in Figure 4. Under sensor-mediated control using relative distance measurements as depicted, the formation graph is both isostatic and acyclic. The formation is not stably rigid, however, because the relative distance between node 2 and node 3 is not directly available from the distributed sensor measurements. Hence, at least one further condition is needed for a sensor-mediated control strategy toproduce a stably rigid formation. We recall the following:

Definition 7 Let $(\mathcal{S}, E)$ be a directed graph. For a vertex $s \in \mathcal{S}$, the *out-valence* of s is the number of incident edges which are directed away from s, and the *in-valence* is the number of edges incident to s which are directed toward s.

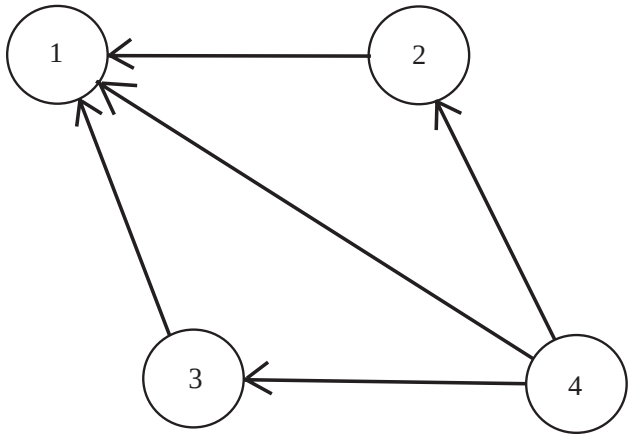

Figure 4: If relative distances are prescribed on the directed edges of this formation graphic, the resulting formation framework is rigidly prescribed. It is not stably rigid, however, as explained in the text.

From Figure 4, it is clear that the presence of a vertex with out-valence 3 causes a problem because when this occurs, none of the other three vertices can have an out-valence greater than 1. This means the relative distance between nodes 2 and 3 cannot be determined by the distributed sensor data alone. This observation suggests our general result:

Proposition 1 *If a formation is stably rigid under the distributed relative distance control (5), then the corresponding formation graph must*

1. *be isostatic,*
2. *be acyclic, and*
3. *have no vertex with an out-valence greater than 2.*

Proof We have already established that the formation graph should be isostatic and acyclic. Hence we turn to the third condition. It was clear in the case of a formation graph with four vertices that this condition is necessary, since otherwise, as illustrated by Figure 4, the graph is not stably rigid based on only local information from distributed sensors. This may be extended to the general case using Laman's theorem, which states that if a graph $(\mathcal{S}, E)$ is isostatic, then the cardinalities of the sets $\mathcal{S}$ and E are related by $|E| = 2|\mathcal{S}| - 3$. (See [8] for a statement and proof of Laman's Theorem.) Suppose some vertex has out-valence ≥ 3. Then among the remaining $|\mathcal{S}| - 1$ vertices, the total out-valence must be $\leq |E| - 3$ (since the total out-valence over all vertices is $|E|$). Now from Laman's theorem, $|E| - 3 = 2|\mathcal{S}| - 6 = 2(|\mathcal{S}| - 3)$. We claim that at least three of the remaining $|\mathcal{S}| - 1$ vertices must have out-valence less than 2. To see this, first notice that at least two of all the vertices must have out-valence < 2, for otherwise the remaining vertices in the graph would exceed $2(|\mathcal{S}| - 3)$ in total out-valence. Label any two vertices having out-valence less than 2 a and b. By the same valence counting argument, we see that if there is no third vertex with out-valence < 2, then both vertices a and b must have out-valence 0, meaning neither could locate it's position relative to the formation. Small perturbations in the relative positions of these nodes would not decay asymptotically, and indeed their motion could in no way be coordinated with the formation. Hence we have established the claim that at least three vertices would have out-valence < 2 under the assumption that at least one vertex in the formation graph has out-valence > 2. But if at least three vertices have out-valence less than 2, then the formation is not stably rigidly positioned with respect to a "leader" and "first-follower." This establishes the proposition. □

The necessary conditions of the proposition are not also sufficient. The formation and sensing pattern depicted in Figure 4 shows that an acyclic isostatic formation graph does not guarantee that the formation is stably rigid. Even adding the requirement that there is a no vertex with out-valence greater than 2 will not guarantee stable rigidity as the following example shows.

Example 1 Consider a formation graph which is isomorphic to the complete bipartite graph K_{33} with the edge orientations as depicted in Figure 5(a). By redrawing the graph as in Figure 5(b), one may verify that just as in the analysis of the configuration of Figure 4, some of the nodes 3,4,5,and 6 do not have their relative positions determined using the distributed distance sensing patterns depicted in the graph. Nevertheless, all the conditions of Proposition 1 are satisfied.

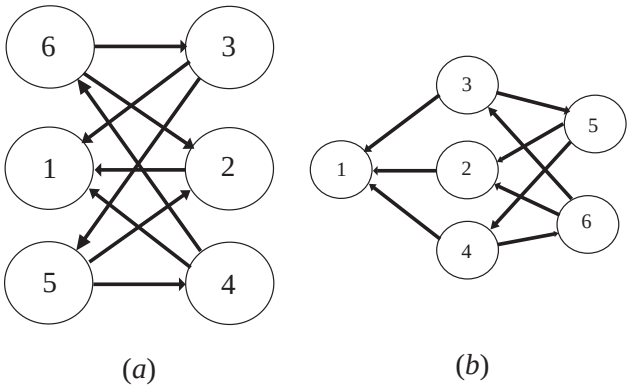

Figure 5: The directed graph depicted here satisfies the necessary conditions of Proposition 1, but it is not stably rigid.

To establish sufficient conditions, we introduce the following useful constructive procedure. Let $(\mathcal{S}, E)$ be a formation graph with vertex set $\mathcal{S} = \{s_1, \ldots, s_n\}$, and $n \geq 2$, and let s_0 be a vertex which is different from

any in $\mathcal{S}$. Further let $\{s_{i_1}, s_{i_2}\}$ be any two vertices in $\mathcal{S}$. The directed graph $(\hat{\mathcal{S}}, \hat{E})$ where $\hat{\mathcal{S}} = \{s_0, s_1, \ldots, s_n\}$ and $\hat{E} = E \cup \{(s_0, s_{i_1}), (s_0, s_{i_2})\}$ with the directions of the added edges being from s_0 to s_{i_j}, is called an *extension* of $(\mathcal{S}, E)$. A corresponding extension to a formation framework $(\mathcal{S}, E, \mathbf{q})$ is called a *rigid extension* if the points $\mathbf{q}(s_0)$,$\mathbf{q}(s_{i_1})$, and $\mathbf{q}(s_{i_2})$ are not collinear.

Theorem 1 *If a formation is constructed from a framework comprised of a single directed edge by a sequence of rigid extensions, then it is stably rigid.*

Proof The proof is a simple inductive construction. We have shown that adding a vertex to a directed edge results in a stably rigid formation framework, provided the added vertex does not correspond to a point which is collinear with the edge. At each stage in the inductive construction, the added vertex will result in a stably rigid formation except in the exceptional case of its being collinear with the two vertex points to which it has been attached. □

Remark 2 Theorem 1 gives the simplest characterization of sensor-based formation rigidity of which we are aware. It shows that there is a close but not exact connection with the classical theory of graph rigidity. It also gives a simple constructive procedure for assembling rigid vehicle formations which has two salient features: (*i*) it is simpler than the classical procedure for constructing rigid (isostatic) graphs, and (*ii*) it can be used to guide the assembly of rigid formations of nonholonomic vehicles, as will be described in Section 5 below. To understand the first of these points, recall that there are two classical procedures for constructing rigid graphs—*extensions* and *edge-splits*. Extensions are essentially the same as what we have called *rigid extensions*. (See [8] for details.) Edge-splits are not of interest to us because they result in vertices of valence three. The main distinction between our construction of rigid formations and the classical constructive theory of rigid planar graphs is highlighted by the following classical result.

Theorem 2 (Henneberg, [8]) *A planar graph is rigid if and only if it may be constructed from a single edge by a sequence of extensions and edge-splits.*

The classical rigid planar graphs which are of interest to us are thus those which can be constructed from a single edge by vertex extensions alone. Some idea of the kinds of graphs which can thus appear is given by considering the problem of enumerating the set of all rigid isostatic graphs on six vertices. There are thirteen in all. Of these, eleven can be constructed by extensions alone, while two (including the complete bipartite graph K_{33}, depicted with directed edges in Figure 5) require edge-splits.

Remark 3 *On formations assembled with reference to a* leader-first-follower *pair.* The constructive characterization of formation rigidity in Theorem 1 suggests that all rigid formations can be assembled by adding vehicles in sequence relative to a fixed *leader-first-follower* pair. Strategies for doing this in the case of large numbers of vehicles remain to be articulated, but as we shall see below, there are control laws even in the case of nonholonomic vehicles for moving a vehicle into position as a rigid extension to a given formation framework.

4 Rigid formations of vehicles subject to nonholonomic constraints

Up to this point, we have confined our discussion to the very simple case of controlling formations using simple line-of-sight distance measurements between idealizations we have called "point vehicles." We are able to tightly couple motion control of such vehicles with a stability theory for graphs because it is always possible to move such vehicles in any direction including those aligned with edges of the formation framework. The theory of stably rigid formation frameworks is more challenging in the case of nonholonomic vehicles .

While several feedback control laws using line-of-sight proximity sensing arise in a very natural way, many do not satisfy Brockett's necessary conditions for asymptotic stabilization, and hence their use must involve care for the stability of the resulting motion and its effect on integrity of the prescribed formation framework. The feedback designs we shall propose are of a simple type in which controls are continuous functions of the system states. While such feedback laws cannot be asymptotically stabilizing in any neighborhood of a desired limiting point, we shall show that asymptotic control objectives can be achieved on all but a thin subset of system states. Understanding the geometry of these subsets is essential to the success of our method of controlling robot vehicle formations.

Our approach is one of several that have been proposed for "hedging" the consequences of Brockett's theorem. In the nonlinear control theory literature of the past decade or so, various techniques for stabilizing systems not satisfying Brockett's necessary conditions have been proposed. These include the use of time-varying controllers (e.g. [4],[17]) and discontinuous control laws ([14]). For a proof and discussion of Brockett's theorem and additional references, see [1].

The present section presents several results of a research program aimed at developing a large catalogue of simple motions which may be implemented by feedback control using "near-neighbor" sensing strategies. Specifically, we analyze three simple controlled nonholonomic motions, each of which can be used in conjunction with other controlled motions to assemble or move a rigid vehicle formation of the type described in Section 3. The three motions are:

- A simple feedback law based on relative distance and bearing measurements to move a nonholonomic vehicle from an "essentially arbitrary" initial configuration to a prescribed location and orientation.
- A simple feedback law of the same type to control a nonholonomic vehicle starting at an "essentially arbitrary" initial configuration to follow a "leader" vehicle which is moving at fixed (but unknown) rates of forward and turning motions, and
- A simple feedback law of the same type to control a nonholonomic vehicle starting from an "essentially arbitrary" initial configuration to approach to within a prescribed distance of a goal location with an orientation prescribed as $+\pi/2$ or $-\pi/2$ with respect to the line-of-sight vector to the goal. This motion can be used in conjunction with a circling motion and a reorientation motion (described elsewhere) to assemble formations of any prescribed geometry (such as the rigid frameworks of the preceding section).

The terminology "essentially arbitrary" here is important, because none of the feedback laws discussed in this section guarantees globally asymptotic motion toward the desired goal configuration. The results below give explicit characterizations of the initial configurations where the control laws break down, and it is shown these sets of configurations are very thin. Each of the control laws is designed with the idea that it will operate within a prescribed region in a vehicle's configuration space and will achieve only a very specific objective (such as move a vehicle to within a prescribed sensed distance of another vehicle). Our overall strategy is to develop a sufficiently rich set of control laws that they can be spliced together to achieve global objectives from actions which are localized in both time and space. The emphasis here is on relative position control (as opposed to global position control). Implicit in the discussion is the assumption that there is a leadership hierarchy (as is suggested by the constructive procedure of Theorem 1). We assume that the global positions and motions of the leader and first-follower are determined in some way, and our focus will be on motions which position other vehicles with respect to those above them in the leader-follower hierarchy.

Motion primitives for assembling vehicle formations: All vehicles under consideration have configuration variables (x, y, θ) as depicted in Figure 1. Motions are assumed to be nonholonomic, and

governed by the equations of motion

$$\begin{pmatrix} \dot{x} \\ \dot{y} \\ \dot{\theta} \end{pmatrix} = \begin{pmatrix} v\,\cos\theta \\ v\,\sin\theta \\ \omega \end{pmatrix}. \tag{6}$$

The control inputs are the vehicle's forward velocity v and turning rate ω, and in each of the motions we discuss, v and ω will be defined in terms of other variables which are directly related to the motion objective and whose values can be determined in real time from sensor data. This simple general model of velocity control does *not* satisfy Brockett's necessary conditions, and therefore none of the control laws which are specializations of (6) will be globally asymptotically stabilizing. Our approach to all the systems under consideration is to use very classical types of constant-gain feedback while carefully keeping track of the restricted spatial domains in which such laws will achieve the desired objectives. The most basic control law of the type we shall consider is the following.

Simple vehicle motion toward a stationary goal frame: We define our control law in terms of the variables depicted in Figure 6. Let (x_r, y_r, θ_r) represent the position and orientation of the goal frame. More specifically, we let ρ be the line-of-sight distance and ϕ the angle relative to the controlled vehicle's frame. These variables correspond to quantities which are readily available from sensor measurements of bearing and relative proximity. In terms of ρ and ϕ, the equations of motion (6) are written

$$\begin{pmatrix} \dot{\rho} \\ \dot{\phi} \\ \dot{\theta} \end{pmatrix} = \begin{pmatrix} -v\,\cos\phi \\ -\omega + \frac{v}{\rho}\sin\phi \\ \omega \end{pmatrix}. \tag{7}$$

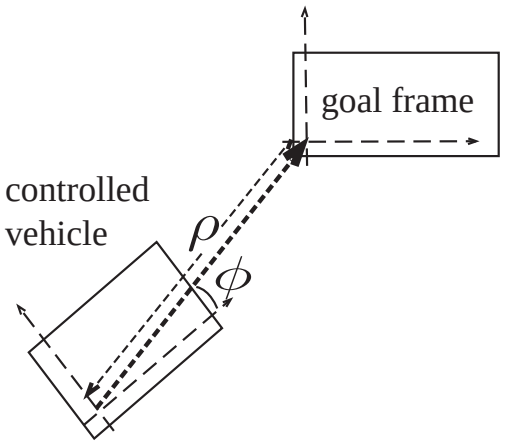

Figure 6: The controlled vehicle measures line-of-sight distance and relative orientation to the goal frame.

We wish to find a feedback law which will steer any initial state (x_0, y_0, θ_0) to the goal state (x_r, y_r, θ_r). Although there is no continuous feedback law which will be globally asymptotically stabilizing, we propose the following feedback law

$$\begin{aligned} v &= k_1\rho, \quad \text{and} \\ \omega &= k_2\phi + k_1\sin\phi, \end{aligned} \tag{8}$$

with the hope of tuning the parameters k_1 and k_2 to meet our motion objectives. Using this v and ω in equation (7), we obtain closed loop equations in which the equation for ϕ becomes:

$$\dot{\phi} = -k_2\phi,$$

so that

$$\phi(t) = \phi_0 e^{-k_2 t},$$

where $\phi(0) = \phi_0$. The equation for ρ becomes

$$\dot{\rho} = -k_1\rho\cos\phi.$$

Since $\phi(t)$ tends exponentially to 0 as $t \to \infty$, ρ also tends asymptotically to 0. Thus, for any choices of $k_1, k_2 > 0$, the pair (ρ, ϕ) is asymptotically stable with $(\rho, \phi) \to (0, 0)$ as $t \to \infty$. The θ component of the equations requires a more detailed analysis. Under this feedback law,

$$\dot{\theta} = k_2\phi + k_1\sin\phi,$$

from which it follows that

$$\theta(t) = \theta_0 - \left[\phi_0 e^{-k_2 t}\right]_0^t - \left[\frac{k_1}{k_2} Si(\phi_0 e^{-k_2 t})\right]_0^t,$$

where $Si(x)$ is the Sine Integral defined by

$$Si(x) = \int_0^x \frac{\sin t}{t}\, dt.$$

We wish to have $\theta(t) \to \theta_r$ as $t \to \infty$, so that

$$\theta_r = \theta_0 + \phi_0 + \frac{k_1}{k_2} Si(\phi_0). \tag{9}$$

From equation (9), we see that the gains need to be chosen to satisfy the ratio

$$\frac{\theta_r - \theta_0 - \phi_0}{Si(\phi_0)} = \frac{k_1}{k_2}. \tag{10}$$

It is also necessary that both k_1,$k_2 > 0$. There are three cases to consider:

Case $-\pi < \phi_0 < 0$. In this case, since Si is an odd function, we must choose the representation of our goal orientation θ_r such that $\theta_r - \theta_0 < \phi_0 < 0$. This will ensure that both $k_1, k_2 > 0$, and the resulting trajectory will have the vehicle turning in the appropriate (clockwise) direction.

Case $0 < \phi_0 < \pi$. In this case, we must chose the representation of our final goal orientation such that $\theta_r - \theta_0 > \phi_0$, and the resulting motion has the vehicle turning monotonically in the counter clockwise direction.

Case $\phi_0 = 0, \pi$. In this case, the vehicle approaches (moves away from) $(x_r, y_r) = (0, 0)$ along the line-of-sight vector $(x_r - x_0, y_r - y_0)$ ($\phi \equiv 0$), and we see that the control law (8) cannot be used to steer the vehicle into the desired configuration.

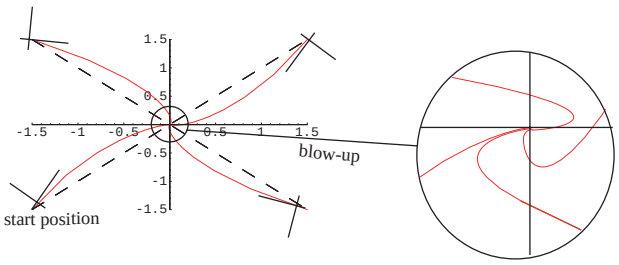

Figure 7: The controlled vehicle starting at four different points on forty-five degree lines and moving to a goal configuration with coordinates $(x, y, \theta) = (0, 0, 0)$. Although it is difficult to see even in the magnified diagram, the vehicle starting in the upper left-hand quadrant must turn through more than $7\pi/4$ radians.

The content of this analysis is illustrated in Figure 7. We plot four motions, starting at four different points which are equidistant from the origin along the diagonal lines indicated. In all cases, the initial heading relative to the line-of-sight to the goal is $\phi_0 = -\pi/10$, so that the vehicles turn in a clockwise direction as they move toward the goal. Since in all cases, the goal configuration has the vehicle's body axes aligned with the given spatially fixed frame, the different initial configurations require different amounts of turning—with the vehicle starting in the lower left-hand quadrant turning the least and the vehicle in the upper left-hand quadrant turning the most. The gains have been chosen so that in all cases $k_1 = 1$ and $k_2 = 0.397813,\ 0.132604,\ 0.0795626$, and 0.0568305 respectively corresponding to the initial conditions in the lower left-hand quadrant and proceeding counter clockwise to the upper left-hand quadrant. Explicit calculation shows that in all cases $(\rho(t), \phi(t), \theta(t)) \to (0, 0, 0)$ as $t \to \infty$, and that $\dot{\rho}/\dot{\phi} \to 0$, so that the curvature of the paths increases as $t \to \infty$. Moreover, the relative rates of increasing curvature are such that the curves never intersect.

Remark 4 *An example of hybrid feedback control.* For any choices of $k_1, k_2 > 0$, ρ and ϕ tend asymptotically to zero. If (10) is satisfied exactly, θ also tends asymptotically to zero. The real-time data needed to realize this control comes from sensor measurements of ρ and ϕ. Our control of θ is accomplished by choosing k_1 and k_2 to satisfy (10), and in principle, this needs to be done only once—before initiating the motion.

Remark 5 *An invariant quantity.* Suppose $(x(t), y(t), \theta(t))$ is a trajectory defined by the above control strategy. Suppose the motion is stopped at some time T, $0 < T < \infty$. We then restart the motion, using the same strategy with

$$\frac{\theta_r - \theta(T) - \phi(T)}{Si(\phi(T))} = \frac{k_1}{k_2}.$$

This ratio must be exactly what it was on the first segment of the trajectory, and this shows that in fact

$$\frac{\theta_r - \theta(t) - \phi(t)}{Si(\phi(t))}$$

is invariant under the motion of (7) with respect to the control (8). This in turn, allows us to write down an equivalent feedback law

$$v = \rho, \quad \text{and}$$
$$\omega = \frac{Si(\phi)\ \phi}{\theta_r - \theta - \phi} + \sin\phi,$$

which, for the proper choice of θ_r representing the goal configuration, will steer (7) asymptotically to $(\rho, \phi, \theta) = (0, 0, \theta_r)$, provided the initial condition $\phi_0 \neq 0$.

Simple vehicle motion toward a moving goal frame: Consider the same sets of variables as depicted in Figure 6. Now, however, we assume the goal frame is moving with forward velocity v_r and turning velocity ω_r, so that the goal-frame equations of motion are

$$\begin{pmatrix} \dot{x}_r \\ \dot{y}_r \\ \dot{\theta}_r \end{pmatrix} = \begin{pmatrix} v_r \cos\theta_r \\ v_r \sin\theta_r \\ \omega_r \end{pmatrix},$$

and the equations of relative motion are

$$\begin{pmatrix} \dot{\rho} \\ \dot{\phi} \\ \dot{\alpha} \end{pmatrix} = \begin{pmatrix} -v\cos\phi + v_r\cos(\phi-\alpha) \\ -\omega + (v/\rho)\sin\phi - (v_r/\rho)\sin(\phi-\alpha) \\ \omega_r - \omega \end{pmatrix}, \tag{11}$$

where α is the relative angle $\alpha = \theta_r - \theta$.

For the control law

$$v = k_1\rho, \quad \omega = k_2\phi, \quad \text{with} \quad k_1, k_2 > 0, \tag{12}$$

the closed loop equations are,

$$\begin{pmatrix} \dot{\rho} \\ \dot{\phi} \\ \dot{\alpha} \end{pmatrix} = \begin{pmatrix} -k_1\rho\cos\phi + v_r\cos(\phi-\alpha) \\ -k_2\phi + k_1\sin\phi - (v_r/\rho)\sin(\phi-\alpha) \\ \omega_r - k_2\phi \end{pmatrix}. \tag{13}$$

When $v_r \neq 0$ the system (13) is no longer of a form whose asymptotic stabilizability is in question because of Brockett's theorem. Given any prescribed motion of the "leader" (v_r, ω_r) it is possible to study stable tracking laws. Here we provide a detailed analysis of the quasi-static case in which the motion of the leader is at constant velocity (v_r, ω_r). In this case there is a unique relative equilibrium configuration with the follower having a constant relative distance and bearing. If $(\rho_0, \phi_0, \alpha_0)$ represents this equilibrium which is obtained by setting $(\dot{\rho}, \dot{\phi}, \dot{\alpha}) = \mathbf{0}$ then,

$$\begin{aligned} \phi_0 &= \tfrac{\omega_r}{k_2}, \\ \alpha_0 &= \phi_0 - \arctan\left(\frac{-\omega_r + k_1\sin\left(\frac{\omega_r}{k_2}\right)}{k_1\cos\left(\frac{\omega_r}{k_2}\right)}\right), \quad \text{and} \\ \rho_0 &= \tfrac{v_r\cos(\phi_0-\alpha_0)}{k_1\cos\phi_0}. \end{aligned} \tag{14}$$

The linearized system about this equilibrium point is given by

$$\begin{pmatrix} \dot{\delta\rho} \\ \dot{\delta\phi} \\ \dot{\delta\alpha} \end{pmatrix} = A(\rho_0, \phi_0, \alpha_0) \begin{pmatrix} \delta\rho \\ \delta\phi \\ \delta\alpha \end{pmatrix} \tag{15}$$

where

$$A(\rho_0, \phi_0, \alpha_0) = \begin{pmatrix} -k_1\cos\phi_0 & v_r\cos(\phi_0-\alpha_0)(\tan\phi_0 - \tan(\phi_0-\alpha_0)) & v_r\sin(\phi_0-\alpha_0) \\ \frac{v_r\sin(\phi_0-\alpha_0)}{\rho_0^2} & -k_2 & \frac{v_r\cos(\phi_0-\alpha_0)}{\rho_0} \\ 0 & -k_2 & 0 \end{pmatrix}. \tag{16}$$

The determinant of $A(\rho_0, \phi_0, \alpha_0)$ is

$$det(A(\rho_0, \phi_0, \alpha_0)) = -k_2(\omega_r^2 - 2k_1\omega_r\sin(\phi_0) + k_1^2) \tag{17}$$

which is non-zero when the reference frame is moving for all choices of k_1, k_2, ω_r, v_r except $k_1 = \omega_r$ and $\phi_0 = \frac{\pi}{2}$.

A striking fact is that the eigenvalues of $A(\rho_0, \phi_0, \alpha_0)$ do not depend on v_r. The characteristic equation of (16) is,

$$\lambda^3 + (k_2 + k_1 \cos\phi_0)\lambda^2 + (-\omega_r k_1 \sin\phi_0 + \omega_r^2 + 2k_1 k_2 \cos\phi_0)\lambda + k_2(\omega_r^2 + k_1^2 - 2k_1\omega_r \sin\phi_0) = 0. \qquad (18)$$

Since (18) is a cubic equation there is always one real root, i.e., $A(\rho_0, \phi_0, \alpha_0)$ will always have one real eigenvalue. Using Routh-Hurwitz criteria it is straightforward to show that the eigenvalues of matrix $A(\rho_0, \phi_0, \alpha_0)$ have negative real part for $k_2 > k_1$. Thus the original non-linear system given by (11) is locally asymptotically stable for $k_2 > k_1$. Two cases are of interest.

When $\omega_r = 0, v_r \neq 0$ the reference frame (lead vehicle) is moving in a straight line. The unique rest point of (13) is given by

$$\begin{array}{rcl} \phi_0 & = & 0 \\ \alpha_0 & = & 0 \\ \rho_0 & = & \frac{v_r}{k_1} = 1 \end{array} \qquad (19)$$

Assuming no saturation for the follower's forward velocity and choosing $k_1 = v_r$ we can ensure that the follower frame stably tracks the reference frame if $k_2 > k_1$. If $k_2 > 4k_1$ then the tracking system is overdamped and for $4k_1 > k_2 > k_1$ it is underdamped.

When $\omega_r \neq 0, v_r \neq 0$, the lead vehicle traces a circular arc of radius, $r_L = \left|\frac{v_r}{\omega_r}\right|$. Because there are no natural physical units for this problem we shall impose a normalization in which $\rho_0 = 1$. The discussion will then be focused on the stability of the tracking motions for the leader circle of various geometries. The unique relative equilibrium point of (13) is given by (16) with $\rho_0 = 1$, and thus

$$v_r = \sqrt{k_1^2 + \omega_r^2 - 2k_1\omega_r \sin\phi_0} \qquad (20)$$

For given reference frame velocities (v_r, ω_r) we can choose the turning velocity gain such that, $k_2 = \omega_r/\phi_d$, where ϕ_d is the desired bearing for the follower frame. We assume that $|\phi_d| < \frac{\pi}{2}$ to guarantee that all eigenvalues of A are in the LHP. Since the leader is moving in a circular arc, to maintain a constant distance

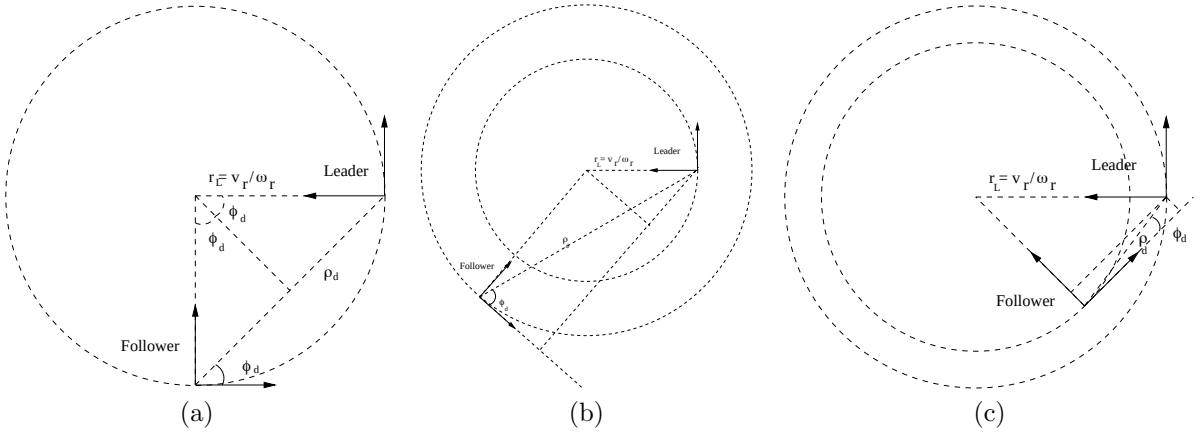

(a) (b) (c)

Figure 8: (a) $\rho_d = 2r_L \sin\phi_d$ - the follower tracks the leader on the same circular arc. (b) $\rho_d > 2r_L \sin\phi_d$ - the follower tracks the leader at a radius bigger than leader's radius. (c) $\rho_d < r_L$ - the follower always tracks the leader at a radius smaller than the leader's radius.

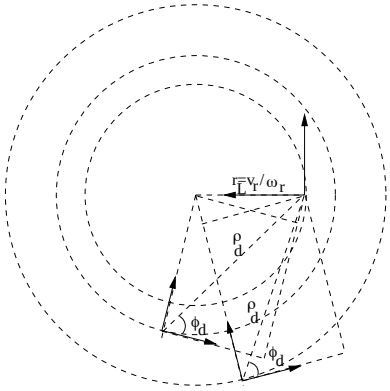

Figure 9: Two leader-follower relative equilibria for $\rho_d > \left|\frac{v_r}{\omega_r}\right| > \rho_d \cos\phi_d$.

and bearing to the leader, the follower also has to move in a concentric circular arc. When the leader's radius of curvature is smaller than 1 this geometric condition is mathematically expressed as, $\cos\phi_d < r_L < 1$. We can also see from Figure 8 that for $\rho_d < 2r_L \sin\phi_d$ the follower's radius is smaller than that of the leader. For $\rho_d > 2r_L \sin\phi_d$ the follower's radius is larger than the leader. Solving (20) for k_1 we get,

$$k_1 = \omega_r \left(\sin\phi_d \pm \sqrt{r_L - \cos^2\phi_d}\right).$$

If $k_1 < k_2$ then the the system (11) is asymptotically stable to $(1, \phi_d, \alpha_0)$. If both values of $k_1 < k_2$ then there are two stable relative equilibria that will stabilize the system to $(1, \phi_d)$ but they will have different relative orientation α as shown in Figure 9. If the leader's radius of curvature is larger than 1 i.e., $1 < r_L$, then solving (20) for k_1 we get the unique stabilizing solution

$$k_1 = \omega_r \left(\sin\phi_d + \sqrt{r_L - \cos^2\phi_d}\right).$$

The choices of gains in (12) can thus be made in a way that ensures stable tracking in this simple setting. Work which will be subsequently reported will provide a detailed analysis of both the qualitative dynamics of tracking a leader whose forward and turning velocities v_r, ω_r are both constant. In addition, we shall discuss the implications of this analysis in terms of tracking leaders whose path velocities are time-varying but subject to curvature constraints.

Simple vehicle motion to a preassigned distance to a goal ending with orientation perpendicular to the line of sight vector: Let ρ and ϕ be the sensor-measured quantities depicted in Figure 6. Let d be a desired distance from the goal point (x_r, y_r) to which we wish to have the robot vehicle approach. Consider the control law $v = \lambda(\rho - d)$, $\omega = \rho\sin\phi - d$ for which the closed loop system is:

$$\begin{pmatrix} \dot{x} \\ \dot{y} \\ \dot{\theta} \end{pmatrix} = \begin{pmatrix} \lambda(\rho - d)\cos\theta \\ \lambda(\rho - d)\sin\theta \\ \rho\sin\phi - d \end{pmatrix}, \tag{21}$$

with $\lambda > 0$ being a suitably chosen feedback gain. In applying this control law, we assume the initial distance $\rho_0 > d$. We then have the following.

Lemma 1 *Along trajectories of (21),*

$$\begin{array}{rcl} \dot{\phi} & = & \lambda(1-\frac{d}{\rho})\sin\phi - (\rho\sin\phi - d), \text{ and} \\ \dot{\rho} & = & -\lambda(\rho - d)\cos\phi. \end{array} \tag{22}$$

The next proposition provides important information characterizing the motions of (21) (or equivalently (22)).

Proposition 2 *The variety*

$$\rho\sin\phi - d = 0$$

is an invariant set for the system (21).

Proof Let x_0,y_0, and θ_0 be initial conditions for (22) such that with

$$\rho_0 = \sqrt{(x_0 - x_r)^2 + (y_0 - y_r)^2}, \text{ and}$$

$$\phi_0 = \arctan(x_r - x_0, y_r - y_0),$$

we have $\rho_0 \sin\phi_0 - d = 0$. Let x,y, and θ evolve according to (21), and let

$$\rho(t) = \sqrt{(x(t) - x_r)^2 + (y(t) - y_r)^2}, \text{ and}$$

$$\phi(t) = \arctan(x(t) - x_0, y(t) - y_0).$$

Introduce the new variable

$$s(t) = \rho(t)\sin\phi(t) - d.$$

The time derivative with respect to t is

$$\dot{s}(t) = \dot{\rho}\sin\phi + \rho\cos\phi\dot{\phi},$$

and from the preceding lemma, it follows that this may be rewritten

$$\dot{s}(t) = -\rho(t)\cos\phi(t)s(t).$$

We thus have the following representation of s:

$$s(t) = e^{-\int^t \rho(\sigma)\cos\phi(\sigma)\,d\sigma} s_0.$$

This proves the proposition, since $s_0 = 0$ implies $s(t) \equiv 0$. □

A further characterization of motions of (21) is given by the following.

Proposition 3 *Suppose the forward velocity gain λ is in the interval $0 < \lambda < d$. Then if the initial value of ρ is given by*

$$\rho_0 = \sqrt{(x_0 - x_r)^2 + (y_0 - y_r)^2},$$

and if we let ϕ_s denote the smallest positive solution of $\phi = \arcsin[d/\rho_0]$, then the set $\phi_s \le \phi \le \pi/2$, $d \le \rho \le \rho_0$ is invariant under the motion of (21).

Proof From Lemma 1,

$$\begin{aligned}\dot{\phi} &= \lambda(1-\tfrac{d}{\rho})\sin\phi - (\rho\sin\phi - d), \text{ and}\\ \dot{\rho} &= -\lambda(\rho-d)\cos\phi.\end{aligned}$$

Clearly $\rho(t)$ is decreasing throughout $d < \rho \leq \rho_0$. Moreover, when $\phi = \phi_s$, $\dot{\phi} > 0$ and when $\phi = \pi/2$, $\dot{\phi} = (\lambda/\rho)(\rho - d) - (r - d) = (\lambda/\rho - 1)(\rho - d) < 0$, under the assumption that $\lambda < d < \rho$. This proves the set is invariant as claimed. □

Consider the function

$$V(\rho,\phi) = \frac{1}{2}\left(\rho\sin\phi - d\right)^2$$

on the invariant set defined in the previous proposition. Differentiating this along trajectories of (21), we obtain (using Proposition 2)

$$\dot{V} = -\rho\cos\phi\,(\rho\sin\phi - d)^2.$$

Since the compact set E characterized in Proposition 3 is invariant, and since solutions of (21) tend in the limit $t \to \infty$ to approach the zero set of $\dot{V}$ (Lasalle's theorem), we conclude that in the asymptotic limit, trajectories must approach either $\cos\phi = 0$ or $\rho\sin\phi - d = 0$. We know from Proposition 1 that $\rho\sin\phi - d = 0$ is invariant under the motion of (21). Moreover, there is no solution (21) such that $\rho\cos\phi \equiv 0$ while $\rho\sin\phi - d \neq 0$.

From the ρ-component of equation (22) we know that in the set E, $\rho(t)$ decreases in the limit to d. The corresponding limit for ϕ must be $\pi/2$, and we have established the following.

Proposition 4 *Suppose the forward velocity gain λ is in the interval $0 < \lambda < d$, and let ρ_0 and ϕ_s be defined as in Proposition 3. Any motion of (21) which starts in the set $E = \{(\rho,\phi) : d \leq \rho \leq \rho_0,\ \phi_s \leq \phi \leq \pi/2\}$ tends asymptotically to $(\rho,\phi) = (d,\pi/2)$. I.e., the vehicle coordinates (x,y,θ) are such that (x,y) tends to a point on the circle*

$$(x - x_0)^2 + (y - y_0)^2 = d^2$$

with the vehicle's body-frame x-axis, $(\cos\theta,\sin\theta)$ tangent to the circle.

While the proposition is immediately useful in terms of designing control laws which will move a vehicle toward tangency with a circle of any radius d about a desired goal point, the hypotheses are actually conservative. Indeed, for any initial condition in which $\rho > d$ and $\rho\sin\phi - d \neq 0$, the corresponding trajectory of (21) tends asymptotically toward the circle as described in the proposition. The essential features of these motions are illustrated in Figure 10. Note that the variety $\rho\sin\phi - d = 0$ has two branches, corresponding to two solution $0 < \phi \leq \pi/2$ and $\pi/2 < \phi < \pi$. These are depicted as green and black curves respectively. On the first of these (green) branches, the motion of the vehicle is asymptotically toward tangency with the circle. On the second (black) branch, the motion is away from the circle. However, these unbounded motions are unstable in the sense that any perturbation will result in a motion which departs and ultimately turns back toward a point of tangency with the circle. Here the set of points which do not lead to trajectories meeting the asymptotic goals of the feedback law is even thinner than in the first simple motion considered above.

Remark 6 A completely symmetric analysis applies to the control law $v = \lambda(\rho - d)$, $\omega = -\rho\sin -d$, for which $\omega = -\rho\sin -d = 0$ is an invariant variety. In this case, almost all trajectories turn toward tangency in the clockwise direction with respect to the goal circle.

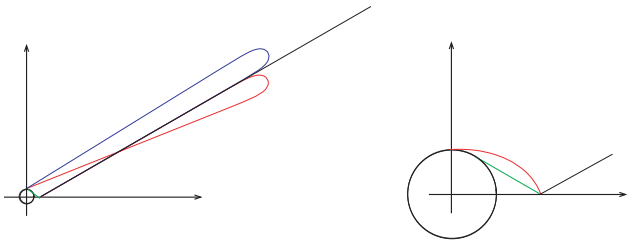

(a) (b)

Figure 10: The feedback control (21) is again *almost* asymptotically stabilizing. Depicted here are several trajectories with initial coordinates $x = 0.5$, $y = 0$, and various values of initial orientation θ. The goal is to move toward a circle of radius 1 centered at $(x, y) = (-1.5, 0)$ with final alignment tangent to the circle, and pointed in the counterclockwise direction of tangency. Figure (a) shows two trajectories in which the initial conditions have the vehicle slightly misaligned in the clockwise (red) and counterclockwise (blue) sense with respect to the unstable branch of the invariant variety $\rho \sin \phi - d = 0$. Figure (b) shows two trajectories near the stable branch of the invariant curve $\rho \sin \phi - d = 0$. Indeed the green trajectory is coincident with this stable branch.

5 Conclusions and preview of further work

We have given a constructive characterization of stably rigid formation frameworks of point vehicles. We have also described three of many possible simple control laws which are of use in assembling and coordinating the motions of formations of nonholonomic vehicles. Although these control laws are not asymptotically stabilizing, we have shown that they do achieve desired objectives asymptotically away from very thin sets of initial conditions which can be described explicitly on a case by case basis. Although there is currently no theory of rigid formations for nonholonomic vehicles, our present research is aimed at understanding how switching rules can be developed for a set of carefully selected control laws in order to achieve formation motions which approximate what can be achieved in the case of point vehicles.

References

[1] A. Bloch, 2003. *Nonholonomic Mechanics and Control* (Interdisciplinary Applied Mathematics, V. 24.), Springer Verlag, New York, March, 2003.

[2] R.W. Brockett, 1990. "Some Mathematical Aspects of Robotics," in *Robotics*, Proceedings of Symposia in Applied Mathematics, Volume 41, American Mathematical Society, Providence, RI, pp. 1-19.

[3] S. Camazine, J.-L. Deneubourg, N.R. Franks, J. Sneyd, G. Theraulaz, and E. Bonabeau, 2001. *Self-Organization in Biological Systems*, Princeton University Press, 538p.

[4] J.-M. Coron, 1991. "Global asymptotic stabilization for controllable systems without drift," Math. Contr. Signals Syst., vol. 5, pp. 295-312.

[5] A. Das, J. Spletzer, V. Kumar, and C. Taylor, "Ad Hoc Networks for Localization and Control," in *Proceedings of the 41-st IEEE Conference on Decision and Control,* Las Vegas, December, 2002, pp. 2978-2983.

[6] T. Eren, P.N. Belhumeur, and A.S. Morse, 2002. "Closing Ranks in Vehicle Formations Based on Rigidity," in *Proceedings of the 41-st IEEE Conference on Decision and Control,* Las Vegas, December, 2002, pp. 2959-2964.

[7] J. Graver,B. Servatius, & H. Servatius, 1993. *Combinatorial Rigidity*, Graduate Studies in Mathematics, vol. 2. American Mathematical Society, Providence, R.I.

[8] J. Graver, 2001. *Counting on Frameworks: Mathematics to Aid the Design of Rigid Structures*, Dolciani Mathematical Expositions, No. 25, The Mathematical Association of America, Washington, DC, 192 pp.

[9] R. Fierro, A.K. Das, V. Kumar, & J.P. Ostrowski, 2001. "Hybrid control of formations of robots," Proceedings of the 2001 IEEE International Conference on Robotics and Automation, Seoul, Korea, May 21-26, pp. 157-162.

[10] L.L. Gould & F. Heppner, 1974. "The vee formation of Canada geese," *Auk*, v. 91, pp. 494-506.

[11] A. Huth & C. Wissell, 1992. "The simulation of the movement of fish schools," *J. of Theoretical Biology*, Vol. 156, pp. 465-485.

[12] E.W. Justh & P.S. Krishnaprasad, 2002. "Equilibria and steering laws for planar formations", submitted to *Systems and Control Letters*, September 2002.

[13] R. Bachmayer & N.E. Leonard, 2002. "Vehicle Networks for Gradient Descent in a Sampled Environment," in *Proceedings of the 2002 IEEE Conference on Decision and Control*, Las Vegas, NV, December, 2002, pp. 112-117.

[14] G.A. Lafferriere & E.D. Sontag, 1993. "Remarks on control Lyapunov functions for discontinuous stabilizing feedback," *Proc. 32nd IEEE Conference on Decision and Control*, San Antonio, TX, 1993, pp. 2398-2403.

[15] F.-L. Lian & R. Murray, 2002. "Real-Time Trajectory Generation for the Cooperative Path Planning of Multi-Vehicle Systems," in *Proceedings of the 2002 IEEE Conference on Decision and Control*, Las Vegas, NV, December, 2002, pp. 3766-3769.

[16] J. Loncaric, 1985. *Geometric Analysis of Compliant Mechanisms in Robotics*, Division of Applied Sciences PhD Thesis, Harvard Univ.

[17] J.B. Pomet, 1992. "Explicit design of time-varying stabilizing control laws for a class of controllable systems without drift," *Syst. Control Lett.*, vol. 18, pp. 147-158.

[18] H.G. Tanner, G.J. Pappas, & V. Kumar, 2002. "Input-to-state stability on formation graphs," in *Proceedings of the 41-st IEEE Conference on Decision and Control,* Las Vegas, December, 2002, pp. 2439-2444.